

RESEARCH ARTICLE

Rapid and High-Throughput Detection and Quantitation of Radiation Biomarkers in Human and Nonhuman Primates by Differential Mobility Spectrometry-Mass Spectrometry

Zhidan Chen,¹ Stephen L. Coy,¹ Evan L. Pannkuk,² Evagelia C. Laiakis,² Adam B. Hall,¹ Albert J. Fornace Jr.,^{2,3,4} Paul Vouros^{1,5}

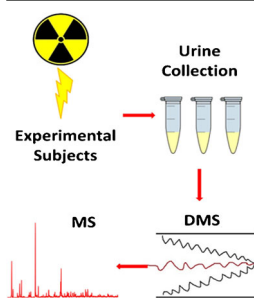
¹Department of Chemistry and Chemical Biology, Northeastern University, Boston, MA 02115, USA

²Department of Biochemistry and Molecular and Cellular Biology, Georgetown University Medical Center, Washington, DC 20057, USA

³Lombardi Comprehensive Cancer Center, Georgetown University, Washington, DC 20057, USA

⁴Center of Excellence in Genomic Medicine Research, King Abdulaziz University, Jeddah, 22254, Saudi Arabia

⁵Barnett Institute of Chemical and Biological Analysis, Northeastern University, Boston, MA 02115, USA



Abstract. Radiation exposure is an important public health issue due to a range of accidental and intentional threats. Prompt and effective large-scale screening and appropriate use of medical countermeasures (MCM) to mitigate radiation injury requires rapid methods for determining the radiation dose. In a number of studies, metabolomics has identified small-molecule biomarkers responding to the radiation dose. Differential mobility spectrometry-mass spectrometry (DMS-MS) has been used for similar compounds for high-throughput small-molecule detection and quantitation. In this study, we show that DMS-MS can detect and quantify two radiation biomarkers, trimethyl-L-lysine (TML) and hypoxanthine. Hypoxanthine is a human and nonhuman primate (NHP) radiation biomarker and metabolic intermediate,

whereas TML is a radiation biomarker in humans but not in NHP, which is involved in carnitine synthesis. They have been analyzed by DMS-MS from urine samples after a simple strong cation exchange-solid phase extraction (SCX-SPE). The dramatic suppression of background and chemical noise provided by DMS-MS results in an approximately 10-fold reduction in time, including sample pretreatment time, compared with liquid chromatography-mass spectrometry (LC-MS). DMS-MS quantitation accuracy has been verified by validation testing for each biomarker. Human samples are not yet available, but for hypoxanthine, selected NHP urine samples (pre- and 7-d-post 10 Gy exposure) were analyzed, resulting in a mean change in concentration essentially identical to that obtained by LC-MS (fold-change 2.76 versus 2.59). These results confirm the potential of DMS-MS for field or clinical first-level rapid screening for radiation exposure.

Keywords: Biomarkers, Radiation exposure, Gamma radiation, Human, Nonhuman primates, Differential mobility spectrometry, Field asymmetric waveform ion mobility spectrometry, DMS-MS, FAIMS-MS

Received: 8 April 2016/Revised: 2 June 2016/Accepted: 16 June 2016/Published Online: 8 July 2016

Introduction

In recent years, the continuing threat of terrorist attacks, and the numerous power industry, industrial, and medical radiological accidents documented in reports by the International Atomic Energy Agency (www.iaea.org), and in scientific literature (for instance, in reports on Fukushima [1]) have drawn attention to radiation injury and to the need for

improved technology for screening and assessing the exposed individuals. Simple and reliable radiation biodosimetry can minimize the public distress after a radiological event by triaging patients and providing medical countermeasures in a timely manner [2–5]. A group of intensive long-term programs directed from Columbia University (see <http://cmcr.columbia.edu>) has extended scientific knowledge of radiation biology and developed rapid diagnostic technologies by taking a three-pronged approach, including classic cytogenetic approaches (micronuclei and gamma-H2AX), transcriptomics, and

Correspondence to: Stephen L. Coy; e-mail: steve.coy@post.harvard.edu, Paul Vouros; e-mail: p.vouros@neu.edu

metabolomics. Brenner et al. [3] have recently given a short overview of diagnostic preparedness and effective countermeasures that includes key references. Although metabolomics is not yet among the available diagnostic tools, it is the most recently developed approach to radiation biodosimetry and recent publications validate metabolomic approaches as simple and highly scalable [6, 7]. Recent work has listed biomarkers with quantified dose-response and identified affected pathways, in cohorts including nonhuman primates (NHP) [8], human total-body-irradiated (TBI) patients [5], and other species such as mouse and rat [9–13]. The efforts are now beginning to expand into targeted analyses based on preceding profiling [14] to provide a deeper mechanistic understanding of radiation response. For clinical and field diagnostics, we are now developing simplified high-throughput targeted analysis of diagnostically-significant metabolites with dose-response specific to radiation exposure in easily accessible biofluids such as urine and blood.

Many analytical platforms have been used for separation and characterization of metabolites. Nuclear magnetic resonance (NMR) was an early popular approach; however, it is limited by slow processing speed and poor sensitivity leading to detecting metabolites primarily present in high abundance [15]. Capillary electrophoresis (CE) in combination with mass spectrometry (CE-MS) is particularly noted for its applicability to the analysis of ionic compounds, but suffers from low sensitivity due to limited sample loading capacity [16]. Gas chromatography (GC)-MS using electron ionization (EI) has been an excellent platform for unambiguous identification of metabolites with the availability of comprehensive mass spectral libraries. However, only thermally stable, volatile, or chemically derivatized metabolites can be analyzed [17]. Liquid chromatography (LC)-MS offers considerable flexibility in that it is not limited to the analysis of thermally stable and volatile compounds and it can deal with many different groups of metabolites. Also due to the different modes of separation mechanisms including reversed phase, normal phase, ion exchange, hydrophilic interaction liquid chromatography (HILIC), chiral, and mixed mode, LC can greatly increase the separation efficiency for each class of metabolites [5, 8, 18–22]. As a result, LC-MS has become a method of choice for metabolite profiling in search of biomarkers related to radiation exposure.

Targeted analyte quantification by LC-MS requires sample cleanup since the variable complexity of biological matrices (e.g., proteins, salts, lipids, acids, bases), can interfere with metabolite signals. Sample purification steps, including protein precipitation, centrifugation, filtration, dilution, and/or solid

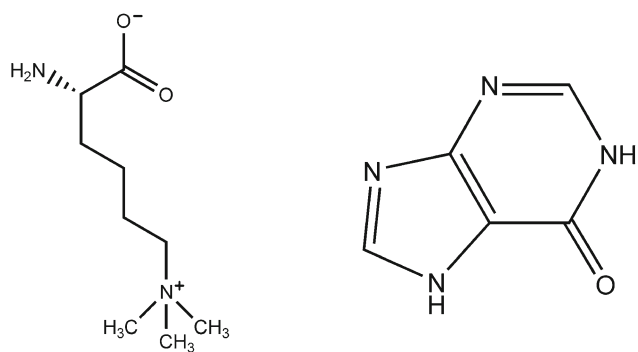
phase extraction (SPE), are thus required prior to LC-MS quantification. However, these additional purification steps add to biomarker analysis time, and this impediment is further compounded by additional chromatographic run time (depending on analyte retention time). These time-consuming processes are not optimal for urgent high-throughput assessment of a large number of individuals exposed to radiation, with some potentially requiring prompt treatment. These considerations necessitate the need for rapid high-throughput biodosimetry methods for assessing radiation exposure.

Differential mobility spectrometry (DMS) in combination with MS (DMS-MS) is an area of considerable in-house activity and has proven to be effective for many applications, including peptide analysis, drugs of forensic interest [7, 23–25], and recently DNA damage biomarker analysis [26]. Here, we investigate DMS-MS as an alternative approach to LC-MS for select biodosimetry biomarkers analysis. DMS offers rapid gas-phase separation/filtration prior to mass analysis, and the advantages of this platform, such as improved signal to noise (S/N) ratio, separation of closely related compounds, and removal of background interferences, have been well demonstrated by a number of groups [7, 23, 26]. Moreover, improved selectivity and, hence, further improvement in S/N ratio can be achieved via the addition of modifiers to the transport gas [27]. Since DMS can preselect ions before MS, it can function as a pre-filter and thus serves as an orthogonal separation technique to MS [28]. The ion filtration time in DMS is only milliseconds and, thus, is no constraint on high-throughput analysis, which is only limited by the rate of sample delivery and sample transfer line clearance [23, 26]. A comparison of analysis times between LC-MS and DMS-MS is summarized in Table 1, showing a clear advantage of DMS-MS over LC-MS for targeted analysis.

Recent studies from our consortium have identified metabolite biomarkers for NHP and human biodosimetry [5, 8, 18], and LC-MS has been used for quantification of several of them. The emergence of radiological terrorism and exposure to radiation in general has highlighted the need for rapid and ideally field and/or on-site deployable methods for identification/quantification of biomarkers indicative of such exposure in biological fluids. As we were arguably among the first to demonstrate the increased speed of analysis of DMS-MS in the analysis of biomarkers in biological specimens at the low ppm level [31–33], we selected two of these compounds, trimethyl-L-lysine (TML) and hypoxanthine (structures shown in Scheme 1), to test the effectiveness of DMS-MS as a viable alternative to LC-MS.

Table 1. Comparison of overall analysis times of LC-MS and manual DMS-MS shows a factor of 10 or more reduction in analysis time using DMS-MS. Development of calibration curves is also faster by about the same factor. Automated flow-injection can further reduce DMS-MS times

Analysis platform	Sample preparation	Detection (including two blanks for carryover elimination)	Overall time (100 samples)
LC-MS	Protein precipitation. 15–25 min for all samples [8, 29] (Low selectivity and clean-up efficiency)	UPLC: 30 min (1 sample, 2 blanks) [29] NanoLC: 60 min (1 sample, 2 blanks) [30]	50–100 h
DMS-MS	Solid phase extraction (SPE) 1–2 h for all samples (high selectivity and clean-up efficiency)	2 min/sample (30 s from sample solution to a stable ESI signal; 30 s for data acquisition; 60 s for cleaning the sample transfer line)	<5.3 h (2 h + 2 min×100)



N_6,N_6,N_6 -Trimethyl-L-Lysine(TML)
 $C_9H_{20}N_2O_2$, m.w. 188.27

Hypoxanthine, $C_5H_4N_4O$
 m.w. 136.11

Scheme 1. Structures of trimethyl-L-lysine and hypoxanthine

Experimental

Chemicals and SPE Cartridges

Formic acid (FA), water, acetonitrile, isopropanol, ethyl acetate (all LC-MS grade), and ammonium hydroxide were purchased from Fisher Scientific (Atlanta, GA, USA); hypoxanthine- $^{15}N_4$ was purchased from Cambridge Isotope Laboratories, Inc. (Andover, MA, USA); hypoxanthine, TML, and TML- 2H_9 were purchased from Sigma-Aldrich (Milwaukee, WI, USA); SCX SPE cartridges (1 mL size) were manufactured by Supelco Inc. (Bellefonte, PA, USA) and purchased from Sigma-Aldrich (Milwaukee, WI, USA) and used for TML; SCX SPE cartridges (1.5 mL size) were manufactured by Grace Davison Discovery Sciences (Deerfield, IL, USA) and purchased from Fisher Scientific (Atlanta, GA, USA) and used for hypoxanthine. Different vendors for the cartridges were used on the basis of their performance to each compound.

DMS-MS Instrumentation

A prototype DMS API 3000 triple quadrupole mass spectrometer (AB SCIEX, Concord, ON, Canada) was used in positive ion mode; the DMS filtration section consists of a simple rectangular region, which has both separation and compensation fields applied when DMS filtration is active, or zero fields when DMS filtration is off (known as “transparent mode”). Our Sciex DMS API 3000 requires considerable disassembly to convert to a non-DMS configuration, and so has been tested only with DMS present. Setting SV and CV fields to zero provides non-selective transmission of all ions regardless of m/z , with the exception of diffusion losses in the DMS section, which at our microspray flow rates may be on the order of 20%–30% [28, 34]. Planar DMS dimensions are 1 mm gap \times 10 mm width \times 15 mm length (H \times W \times L). The separation voltage (SV) ranges from 0 to 5000 V, and the compensation voltages (CV) from -100 to $+100$ V. SV is applied as a two-harmonic waveform difference between 6 and 3 MHz waveforms [35], with the magnitude given as the signed difference between the minimum and maximum voltage applied across the 1 mm gap, so that a setting of 4500 V corresponds to a peak of $+3000$ V/

mm followed -1500 V/mm (when CV = 0 V), as illustrated in Kafle et al. [27]. Ionization used an ESI voltage of $+3500$ V ($+2500$ V difference between emitter and curtain plate), using a stainless steel emitter, 30 μ m i.d., 50 mm length from Thermo Electron North America LLC (West Palm Beach, FL, USA). A syringe pump from Harvard Apparatus (Holliston, MA, USA) was used to infuse the sample at 300 nL/min. The SCIEX micro-spray emitter holder provided N_2 nebulizing at 1000 cc/min. The SCIEX curtain gas flow of 1000 cc/min was heated to 85 $^{\circ}C$, so that both the DMS transport gas and the 400 cc/min curtain gas counter-flow for ion desolvation were both maintained at that temperature. The vacuum drag of the API 3000 was measured to be 600 cc/min. In positive ion mode, the voltage on the curtain plate is fixed at $+1000$ V so that the net emitter potential is 3500 V $-$ 1000 V = 2500 V. The voltage of the DMS filter section is offset by a few volts from the instrument orifice plate for best ion transmission. The gas modifiers used were 1% isopropanol v/v for TML, 0.25% ethyl acetate v/v for hypoxanthine. The optimized SV values were 4000 V for TML and 2000 V for hypoxanthine (such a big difference is probably due to the different thermal stability of the two compounds under field heating), using CV -5 V for TML, -3 V for hypoxanthine. The peak-peak SV setting of 4000 V, when CV is zero, corresponds to a positive peak field of 2667 V/mm and a negative field of -1333 V/mm across the 1 mm gap. At a DMS transport gas temperature of 85 $^{\circ}C$, the E/N value in Townsends of the 4000 V setting corresponds to a peak value of 130 Td, and the 2000 V setting used for hypoxanthine to a peak value of 65 Td. Townsend values are important when considering scaling with atmospheric pressure [36], but are not sufficient by themselves to specify DMS conditions. It is necessary to report the bulk temperature of the DMS transport gas in addition to the field value (field intensity in kV/cm and atmospheric pressure, or field intensity, in Td). That bulk temperature is essential for theoretical modeling of the DMS effect because of a divergence in the influences of temperature and gas density is known from Krylov’s work [37] and work of Kafle et al. [27]. Gas modifiers were introduced to the curtain gas by a syringe pump and went through a 50 $^{\circ}C$ heated metal tube connected to the curtain gas inlet so that the organic solvent was completely evaporated. The percentage of the gas modifier in the curtain gas was calculated by liquid delivery rate, liquid density, and the ideal gas law [23].

Urine Samples

NHP urine samples were stored at -80 $^{\circ}C$ after overnight shipment from Georgetown University. The tested samples were a subset from a full NHP study (CiToxLAB North America, Laval, Canada), specifically three control samples and three exposed/irradiated samples collected 7 d after exposure to 10 Gy. The Institutional Animal Care and Use Committee approved strict criteria for the use of NHPs. Additional information on collection/treatment of these samples has been previously described [8, 38]. Briefly, six male rhesus monkeys were involved for this batch of samples, three were treated with

10 Gy using a ^{60}Co gamma source; the other three were treated as controls and received the same handling, but no irradiation. Urine samples were collected from all groups on d 7 after irradiation and stored at $-70\text{ }^{\circ}\text{C}$.

SCX-SPE Protocols for TML and Hypoxanthine

TML Urine samples were diluted 5-fold with pH 2 water (adjusted with FA). Supelco SCX-SPE cartridges were conditioned with 1 mL pH 2 water, then 200 μL diluted urine samples were applied to each cartridge followed with 1 mL pH 2 water for washing, then followed with 1 mL pH 11 (adjusted with ammonium hydroxide) water for eluting. All eluted samples were dried down by speed-vac at $50\text{ }^{\circ}\text{C}$ and reconstituted in 200 μL 50% acetonitrile + 0.1%FA.

Hypoxanthine Urine samples were diluted 5-fold with pH 2 water (adjusted with FA). Grace SCX-SPE cartridges were conditioned with 1 mL pH 2 water, then 200 μL diluted urine samples were applied to each cartridge and washed with 1 mL pH 9 water (adjusted with ammonium hydroxide), then eluted with 1 mL pH 11 water (adjusted with ammonium hydroxide). All eluted samples were dried down with speed-vac under $50\text{ }^{\circ}\text{C}$ and reconstituted with 500 μL 50% acetonitrile + 0.1%FA.

Sample Preparation for Calibration Curves

All blank urine samples were acidified to pH 2 with FA, stored at $4\text{ }^{\circ}\text{C}$. Normal species TML and hypoxanthine solutions were spiked into acidified blank urine to prepare a series of concentrations: 3.6–927 μM for TML and 35–500 μM for hypoxanthine. Deuterated internal standards were spiked into each sample to bring its concentration to 65 μM for TML samples and 50 μM for hypoxanthine samples. All samples were then diluted 5-fold with pH 2 water, and 200 μL of each sample was used for SPE sample loading. Diluted samples were extracted by the protocols mentioned above.

Sample Preparation for TML and Hypoxanthine Validation Test

TML standard was spiked into acidified blank urine to the following concentrations: 3.6, 7.2, 14.5, 29, 58, 116, 232, and 464 μM , respectively. TML- $^2\text{H}_9$ internal standard was spiked into each sample at a concentration of 65 μM . All samples were then diluted 5-fold with pH 2 water. Two hundred μL of each sample was used for SPE sample loading. Diluted samples were extracted with Supelco SCX SPE followed by the protocol mentioned above.

Hypoxanthine standard was spiked into acidified blank urine to the following concentrations: 20, 35, 50, 100, 200, 350, and 500 μM , respectively. Hypoxanthine- $^{15}\text{N}_4$ internal standard was spiked into each sample at a concentration of 50 μM . All samples were then diluted 5-fold with pH 2 water. Two hundred μL of each sample was used for SPE sample

loading. Diluted samples were extracted with Grace SCX-SPE followed by the protocol mentioned above.

The validation test of the calibration curve was done by a single operator. A new set of samples was prepared as mentioned above, but analyzed unidentified, and in random order. After the analysis was done, the concentrations were back-calculated from the calibration curve for comparison with the prepared concentrations to determine the reproducibility or accuracy of the calibration curve.

Sample Preparation for NHP Urine Samples

Forty μL of each NHP urine sample (three controls and three exposed) were spiked with hypoxanthine- $^{15}\text{N}_4$ to a final concentration of 50 μM . All samples were then diluted 5-fold with water adjusted to pH 2 by the addition of 10 μL FA. Diluted samples were extracted with Grace SCX-SPE followed by the protocol mentioned above. Human samples could not yet be analyzed because of a delay in IRB approval, but validation tests in human urine were performed using the previous preparation.

Data Processing

All data were acquired by Analyst (ver. 1.5.2) and processed by Excel. The signal intensities of both analytes (hypoxanthine and TML) and internal standards (hypoxanthine- $^{15}\text{N}_4$ and TML- $^2\text{H}_9$) were recorded. The intensity ratio of analyte/internal standard was calculated as Y value, the concentration of spiked analytes was calculated as X value to generate calibration curves. For validation tests and NHP urine samples, the detected intensity ratio of analyte/internal standard was then applied into the calibration curve as the Y value. The corresponding X value (concentration, μM) was calculated.

Results and Discussion

Sample Preparation

Although more than 90% of urine consists of water [39], the presence of proteins, lipids, salts, drugs, and other compounds necessitates some form of sample cleanup to minimize ion suppression. Given its simplicity, SPE was selected as a viable option and proved to be ideal for target analyte purification and removal of the bulk of interferences. Despite the current longer time requirement, which can be improved by using a high efficiency speed-vac system, we found the SPE approach preferable to “protein precipitation/dilution” used in the LC-MS analysis [5, 8] because of its high selectivity, compatibility with automation, lower susceptibility for clogging of the sample transfer line, and reduced contamination of the MS. Another advantage of SPE is that it can be developed as a universal sample preparation method for most metabolites since many of the metabolites are polar and ionic. For example, a mixed mode SPE (ion exchange/reversed phase) such as SCX/C18 can retain most of the metabolites and subsequently elute the target

metabolites using appropriate solvents accordingly. In the present study, SCX-SPE was used for both TML and hypoxanthine.

Reduction of Chemical Background and Chemical Noise Using DMS-MS

In the lower mass range, atmospheric pressure ion sources are known to generate ions from background species, and chemical noise from fragments at every unit mass interval [40], but this competing signal is greatly reduced by DMS. In order to assess the selectivity and ability of DMS-MS to increase the signal in the analysis of the selected biomarkers, two spiked samples (60 μM + 65 μM of TML and TML- $^2\text{H}_9$, and 500 μM + 50 μM of hypoxanthine and hypoxanthine- $^{15}\text{N}_4$) were chosen and extracted by SCX-SPE as described in the [Experimental](#) section. Each sample was analyzed by DMS-MS both in the DMS-transparent and DMS-on modes using isopropanol and ethyl acetate as modifiers in each case. The process of optimizing a DMS-MS analysis has been previously reported by our group [26, 27]. Briefly, different organic solvents (gas modifiers) such as isopropanol, ethanol, ethyl acetate, and trifluoroethanol, and their concentrations in the transport gas

were tested to give the best intensity and background removal for analysis of targeted ions under different separation voltages. The optimal gas modifier conditions and SV were set and the CV was scanned. The CV corresponding to the apex of the target ion chromatogram was chosen as the optimal CV for each compound. Only the target ion and very few other background and interfering ions are transmitted when the DMS is on at this stage. In DMS-transparent mode, the separation field and compensation field are zero, whereas in DMS-on mode, the fields are applied for ion selection. The spectra are shown in Figure 1. As is clearly evident, in the absence of DMS application the signals of both TML and TML- $^2\text{H}_9$ are highly obscured, and the entire spectrum is dominated by other interferences and background noise. However, upon setting the separation voltage to 4000 V and fixing the compensation voltage to -5 V (the same compensation voltage was used for both TML and TML- $^2\text{H}_9$) and also introducing 1% isopropanol into the transport gas as a modifier, the intensities show approximately a 2-fold increase for both TML (from 1.27×10^5 to 2.34×10^5) and TML- $^2\text{H}_9$ (1.19×10^5 to 2.85×10^5). An unexpected excess intensity is seen for hypoxanthine- $^{15}\text{N}_4$ in DMS-transparent mode. Because DMS-transparent mode passes ions of all m/z unselectively, it is likely that the excess intensity in DMS-transparent

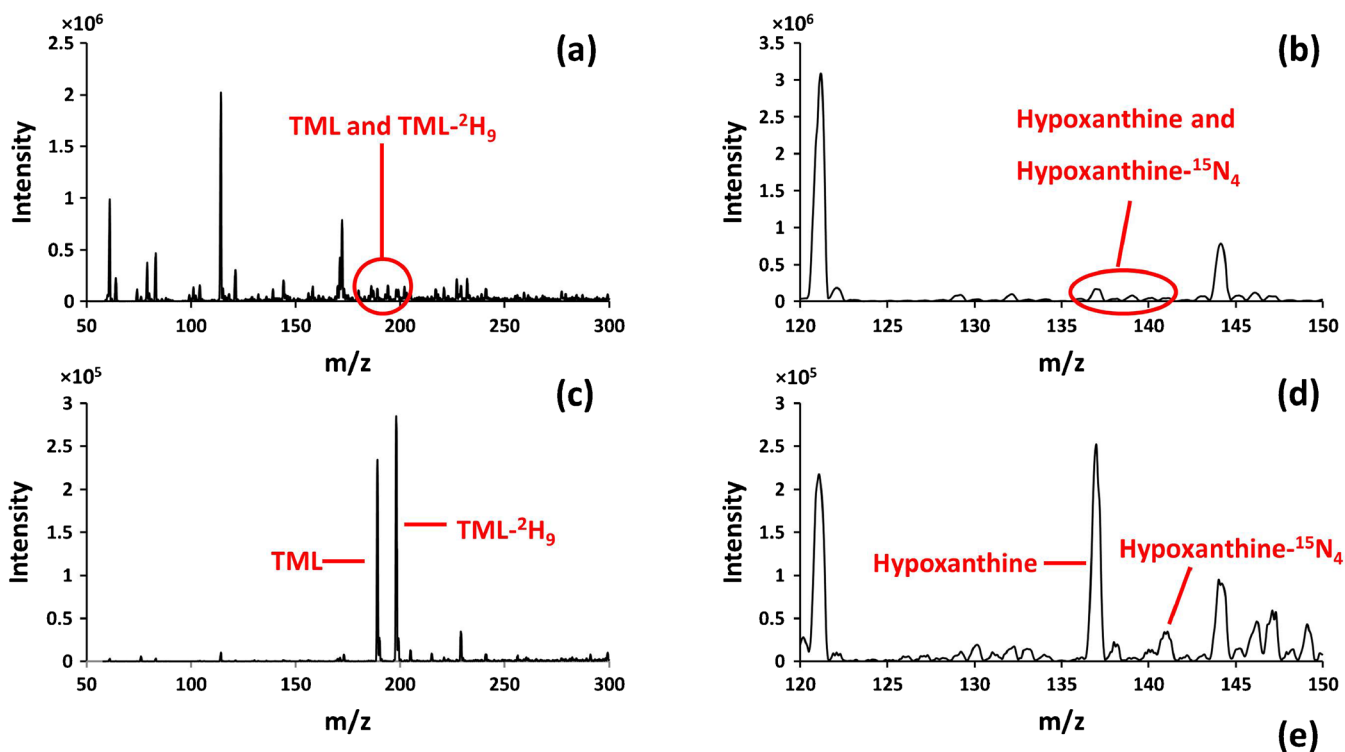


Figure 1. Comparison of the signal and background noise between DMS-transparent (DMS filtration off) and DMS-on mode with optimized modifier concentrations. (a) DMS-transparent mode for TML (m/z 189) and internal standard TML- $^2\text{H}_9$ (m/z 198); (b) DMS-transparent mode for hypoxanthine (m/z 137) and internal standard hypoxanthine- $^{15}\text{N}_4$ (m/z 141); (c) DMS-on for TML and TML- $^2\text{H}_9$ (isopropanol modifier); (d) DMS-on for hypoxanthine and hypoxanthine- $^{15}\text{N}_4$ (ethyl acetate modifier); (e) Table of the intensities of DMS-transparent mode and DMS-on mode; (*) see text for discussion

mode for hypoxanthine- $^{15}\text{N}_4$ is due to an interfering ion that is removed when DMS ion filtration is on. The other DMS-transparent entries in the table did not encounter chemical noise at their exact m/z values. Or in other words, there might be some interferences coexisting with hypoxanthine- $^{15}\text{N}_4$ under DMS-transparent mode and showing a superimposed signal, which was then removed under DMS on mode because of its separation capability. Even more significant, however, is the removal of almost all background interferences and the dramatic increase in contrast for both TML and TML- $^2\text{H}_9$, making them the base peak ions in the spectrum. As discussed in prior publications, this can be explained by changes in clustering-declustering behavior between analyte ions and gas modifiers, which changes the optimal SV and CV for their transmission through the DMS field for MS detection [27, 28, 41, 42]. It is usually found that increasing the separation voltage value from zero to values that provide DMS filtration actually increases the MS signal above the DMS-transparent level. This effect is likely due to enhanced ion desolvation attributable to heating by the DMS fields as described in Kafle et al. [27] and improved solvent declustering and some additional ion-focusing. The

increased transmission is often on the order of a factor of two in intensity. We report optimized analytical results in this paper, omitting investigation of additional intensity effects. Moreover, it is clearly shown in Figure 1a and c that the signal to noise ratio (S/N) was dramatically increased with the removal of the background noise, which can further improve the detection limit. This improvement was not quantified because endogenous levels were generally not observable without DMS.

Quantitation of TML and Hypoxanthine in Urine and the Verification of Quantitation Accuracy by Analysis of Randomized Samples

Optimized conditions for transmission, separation, and detection of TML and hypoxanthine by DMS-MS were investigated next in terms of applicability in human and NHP urine biomarker quantification, a matrix extensively explored in metabolomic biosimetry studies. Since there is no available data for the endogenous level of hypoxanthine in NHP, we used as reference point the normal endogenous levels of TML and hypoxanthine

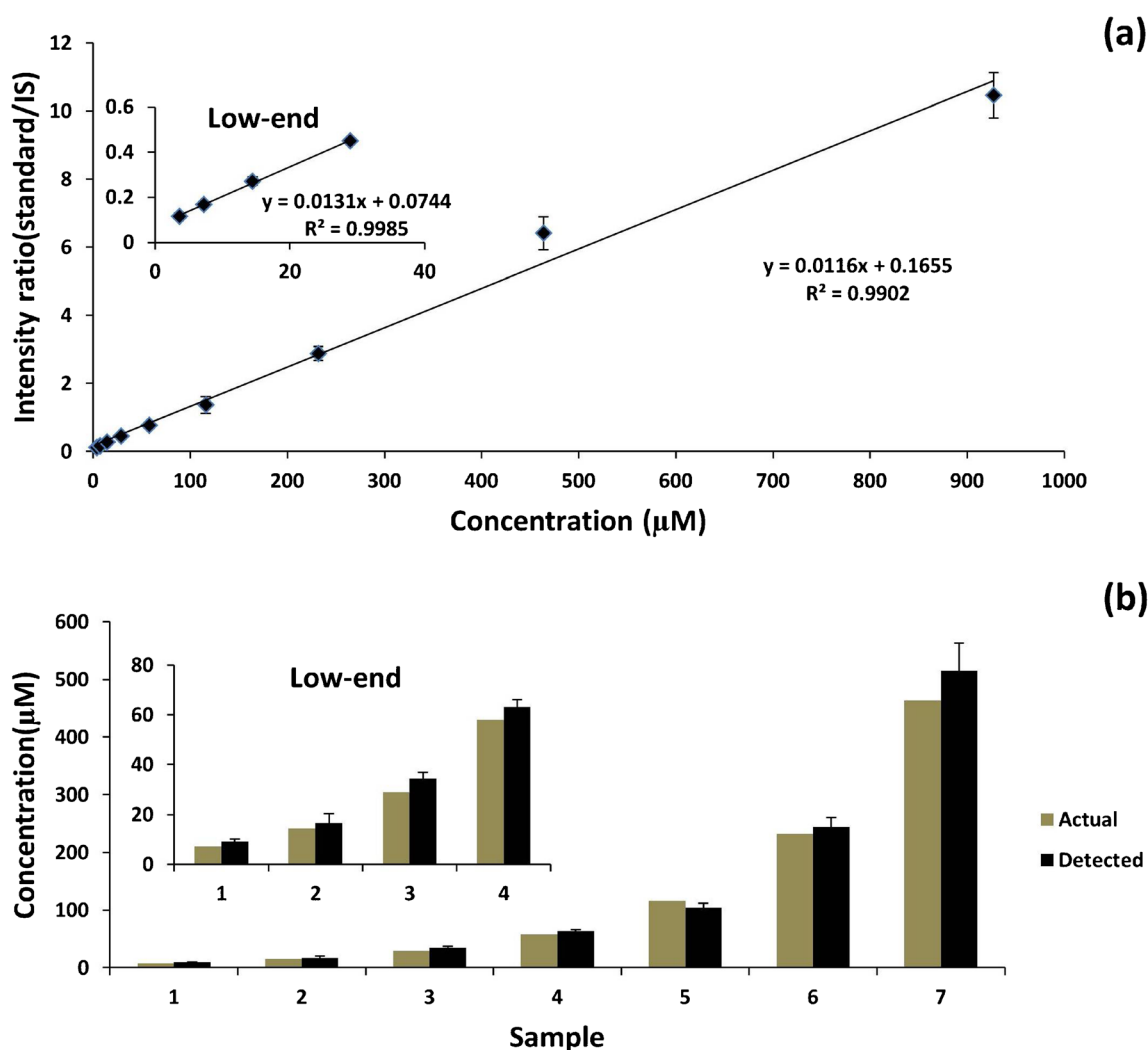


Figure 2. Calibration curve and validation test for accuracy of TML. **(a)** Calibration curve of TML spiked into human urine (3.6 μM –927 μM), error bar is one standard deviation (1σ); **(b)**: validation test of TML, gray column is the actual concentration spiked into urine, black column is the experimental detected concentration, error bar is (1σ)

in human urine. (<http://www.hmdb.ca/metabolites/HMDB01325> and <http://www.hmdb.ca/metabolites/HMDB00157>) It was ascertained that normal TML and hypoxanthine concentrations in human urine are on the order of 30 μM , depending on diet and other individual differences. Concentrations of TML and hypoxanthine in human and NHP irradiated groups are typically elevated less than 10-fold above those in the control groups [5, 8]. As a result, calibration curves were sufficiently constructed to cover the dynamic range for experimental samples (5–500 μM) (Figures 2a and 3a).

Importantly, time consumed to generate individual calibration curves was under 2 h, whereas a time ranging from 12 h (UPLC)[29] to 2 d (NanoLC)[30] is required using LC-MS methods, depending on LC speed due to the duration of LC runs including the clear-down (blank) runs between standards. This large difference is attributed to the replacement of LC runs by the millisecond ion residence time in DMS, which reduces analysis time to the sample delivery rate. Even under manual operation, sample delivery rate can be accomplished in a matter of seconds. In this DMS-MS method, the time spent on each sample is 2 min, which includes 30 s for picking up the sample solution to syringe and forming a stable ESI signal, 30 s for data acquisition, and 60 s for cleaning the sample transfer line.

In order to establish the reliability and accuracy of the DMS-MS procedure in a biological matrix, a series of samples spiked with TML, hypoxanthine, and their respective internal standards was prepared in blank human urine. Biomarker concentrations in those samples covered almost the entire range of the calibration curve in order to evaluate the overall accuracy of the developed protocol. Comparisons between experimental and actual values for the analysis of TML and hypoxanthine are shown in Figures 2b and 3b, respectively. Relative error in samples 1 through 7 of TML is 25.7%, 14.0%, 18.5%, 9%, –10.5%, 5.4%, and 11.0%, respectively. Absolute value of relative error in the seven data points has an average of 10.5%. Relative error in samples 1 through 5 of hypoxanthine is 29.2%, 20.2%, 2.5%, –7.4%, and –6.3%, respectively. Absolute value of relative error in the five data points has an average of 13.1%, showing that DMS-MS analysis has accuracy as high as $90\% \pm 11\%$ (TML) and $87\% \pm 11\%$ (hypoxanthine). Relative error in TML and hypoxanthine validation tests may arise from a number of experimental effects. However, the achieved accuracy of 90% and 87% is adequate at this stage to confirm DMS-MS feasibility and reliability for assessing radiation exposure based on hypoxanthine in NHP samples and TML in human samples.

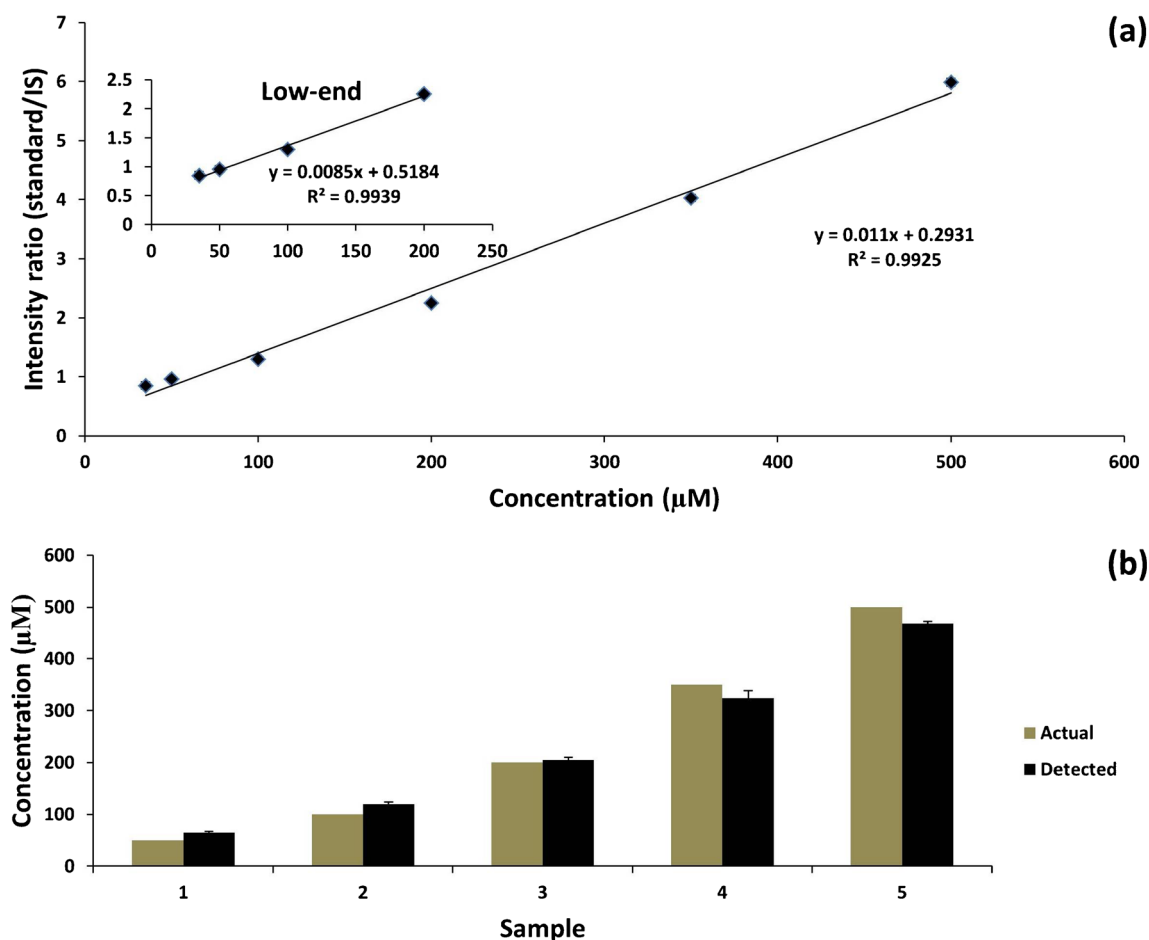


Figure 3. Calibration curve and validation test for accuracy of hypoxanthine. **(a)** Calibration curve of hypoxanthine spiked into human urine (35 μM –500 μM), error bar is (1 σ), but technical replicates were highly consistent; **(b)** validation test of hypoxanthine, gray column is the actual concentration spiked into urine, black column is the experimental detected concentration, error bar is (1 σ)

Hypoxanthine Level in NHP Urine Samples

Evolutionarily, NHPs are the closest widely used animal model to humans and are humanely/ethically used to estimate human response to radiation exposure. In order to show the equivalence of our method to traditional LC-MS, we compared results obtained by DMS-MS versus LC-MS (obtained at Georgetown

University) [8] (Figure 4). To compare DMS/LC results within the NHP urine matrix, but preserve valuable samples for later protocol development, we worked with a subset of NHP samples (male, three controls and three exposed), with the exposure level at the highest dose of 10 Gy. This exposure level was found to have the highest hypoxanthine fold-change compared

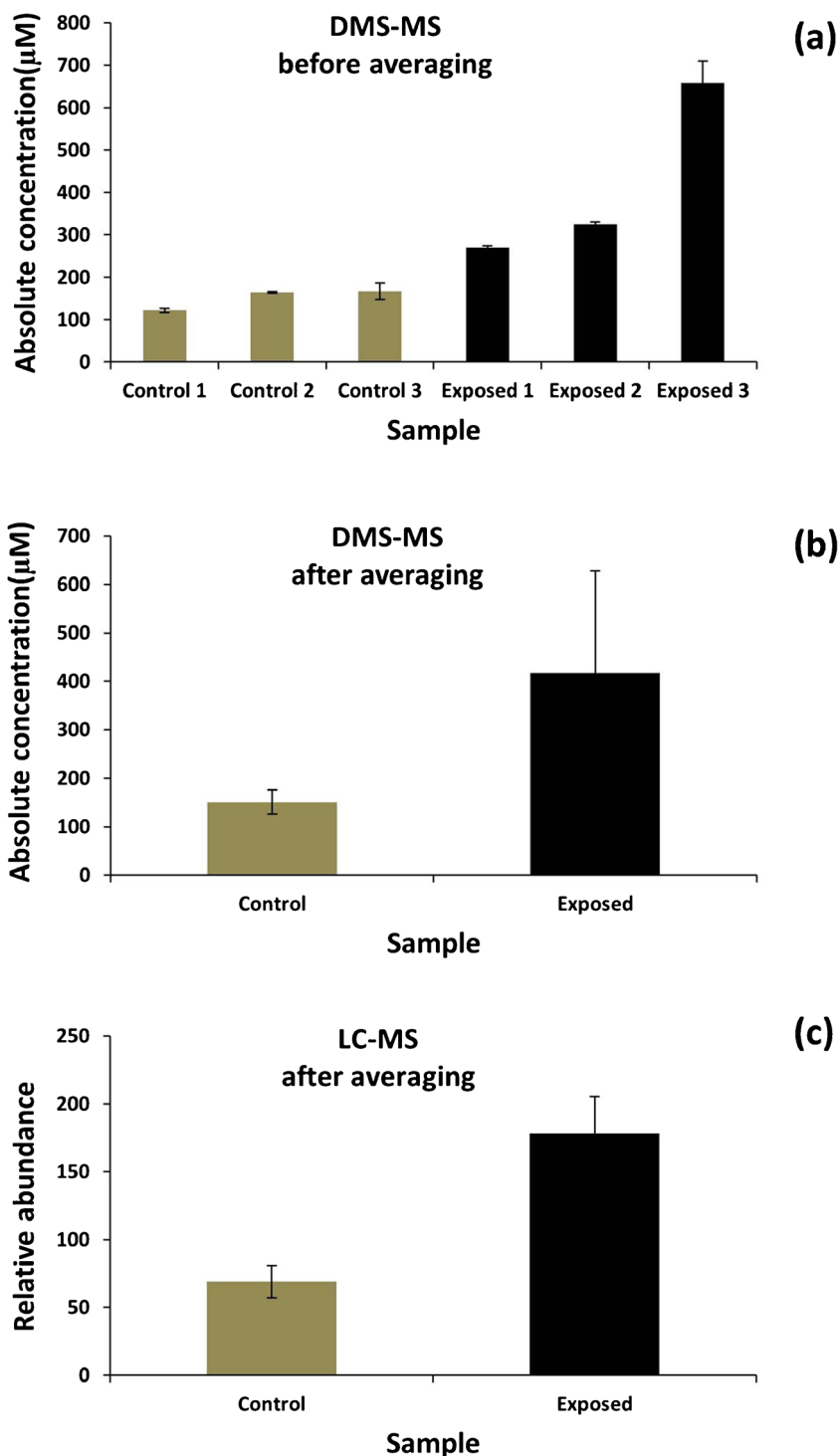


Figure 4. Hypoxanthine level in NHP urine. Control and exposed groups are labeled and color-coded. **(a)** Results obtained from DMS-MS before averaging; **(b)** results obtained from DMS-MS after averaging; **(c)** results obtained from LC-MS after averaging. The difference in the bar heights gives the change in hypoxanthine level in NHP urine due to 10 Gy exposure. Error bars are (1 σ)

with the control group, whereas TML was not found to be a NHP biomarker. Examining individual results, control-group hypoxanthine level is clearly lower than in the exposed group. On averaging, the hypoxanthine level is found by DMS-MS to increase by a factor of 2.76. The fold-change determined by LC-MS was initially reported at 2.4 [8] but has recently been updated to 2.59. This indicates that SCX-SPE followed by DMS-MS is approximately equivalent to LC-MS in this application. We also found from examining the standard deviation of the mean that technical replicates using DMS-MS methodology were highly reproducible. The individual variation of DMS-MS is higher than LC-MS, but this could be due to the degradation of the urine samples during long periods of storage, since additional freeze-thaw cycles from the original analysis have occurred, changing concentrations and modifying ion suppression and carry-over effects. Alternative stabilizing methods of storage and transmittal, such as dried urine spots (DUS), have been reported, and may have advantages over cryogenic storage of liquid biofluid samples (especially for polar, water-soluble, target compounds) [43–45]. Introducing flow injection rather than using direct infusion can help eliminating/decreasing the carry-over effects.

The time spent on analyzing the six NHP samples was <1 h for DMS-MS, whereas ~3–6 h would be required for similar LC-MS analysis. The time required to create a calibration curve for DMS-MS (<2 h) is also much shorter than that required for LC-MS, as previously mentioned. Although the identity of hypoxanthine was confirmed in the LC-MS work at Georgetown University, quantitation was not performed by UPLC-Q-TOF methods at Georgetown because of the extra time and expense. In addition, DMS-MS, for which calibration curves can be rapidly generated, measured the concentrations of hypoxanthine in NHP urine ($150 \pm 20 \mu\text{M}$ for control group and $417 \pm 210 \mu\text{M}$ for the 10 Gy irradiated group), a result not previously available. The absolute concentration ($150 \pm 25 \mu\text{M}$) of hypoxanthine in the control NHP urine as measured by DMS-MS is higher than reported for humans (from The Human Metabolome Database (www.hmdb.ca) human urine, about $5 \mu\text{mol}/\text{mmol}$ creatinine or about $30 \mu\text{M}$, typically).

Conclusion

The development of targeted analytical methods for metabolic biomarkers is of high current interest because of the increasing identification of biomarkers with useful dose-response behavior. The FDA provides guidelines for the development and validation of assays with known accuracy, precision, and recovery [46, 47]. In addition, longitudinal studies are now appearing that verify the consistency of biomarker-panel baseline measurements on individuals over periods as long as 2 y [48], with better performance seen for fasting samples over non-fasting.

In this study, we begin the development of methods to be applied to high-throughput radiation biodosimetry based on targeted metabolomics of urine samples. DMS-MS has been applied to quantitation of two small molecules (TML and hypoxanthine), comprising water-soluble analytes in biological samples that have been selected in recent studies for their association with radiation exposure and biological relevance. When preceded by an efficient and effective SCX-SPE sample preparation, the combined methods provide a rapid and accurate method of detection and quantitation of hypoxanthine and TML in urine matrices. DMS-MS has distinctive advantages for this type of analysis [7], which include suppression of chemical noise and the ability to resolve mixture components from interferences on a continuous basis in milliseconds, bypassing more time-consuming chromatographic separation steps. As shown in Figure 2, the construction of a standard curve comprised of nine calibration points each determined in triplicate, with additional timing for cleaning the sample transfer line, was completed in less than 2 h. This is much less time than is required to prepare a calibration curve by LC-MS, where, in addition to the time consumed for the chromatographic analysis, there is the time associated with column equilibration between runs and several additional blanks to correct for any carryover. The use of appropriate modifiers in DMS-MS (isopropanol and ethyl acetate in this case) tunes the DMS analyte bands to a region free of interferences, and suppresses interferences of low charge affinity, thereby reducing the number of sample cleanup steps. After SPE, the rate determining step for the analysis is essentially the time required for sample delivery and forming a stable ESI signal.

With these supporting results, we look forward to the development of complete, validated protocols for screening-quality radiation biodosimetry based on metabolomics that will be available for subjects exposed to radiological hazards, from specific short-term events to the decades-long hazard of Fukushima or Chernobyl significant residual contamination. Continued methods development will be based on more complete species and time-course response data, further refinement of sample storage and extraction methods, introducing an automated flow injection device, standardization and automation of mass-spectrometric techniques, and continued attention to new bioinformatic methods [49, 50]. The gains in sample throughput are to a large extent specific to the analytes described in this paper. However, they are likely applicable more generally to the analysis of targeted analytes in a broader field of small-molecule bioanalysis.

Acknowledgments

P.V. and A.F. gratefully acknowledge support from NIH (NIAID) R01AI101798 and NIH(NIAID) U19AI067773.

References

1. Normile, D.: Slow bum. *Science* **351**, 1018–1020 (2016)

2. Hafer, N., Cassatt, D., Dicarolo, A., Ramakrishnan, N., Kaminski, J., Norman, M.K., Maidment, B., Hatchett, R.: NIAID/NIH radiation/nuclear medical countermeasures product research and development program. *Health Phys.* **98**, 903–905 (2010)
3. Brenner, D.J., Chao, N.J., Greenberger, J.S., Guha, C., McBride, W.H., Swartz, H.M., Williams, J.P.: Are we ready for a radiological terrorist attack yet? Report from the centers for medical countermeasures against radiation network. *Int. J. Radiat. Oncol. Biol. Phys.* **92**, 504–505 (2015)
4. Patterson, A.D., Lanz, C., Gonzalez, F.J., Idle, J.R.: The role of mass spectrometry-based metabolomics in medical countermeasures against radiation. *Mass Spectrom. Rev.* **29**, 503–521 (2010)
5. Laiakis, E.C., Mak, T.D., Anizan, S., Amundson, S.A., Barker, C.A., Wolden, S.L., Brenner, D.J., Fornace Jr., A.J.: Development of a metabolomic radiation signature in urine from patients undergoing total body irradiation. *Radiat. Res.* **181**, 350–361 (2014)
6. Coy, S.L., Cheema, A.K., Tyburski, J.B., Laiakis, E.C., Collins, S.P., Fornace Jr., A.: Radiation metabolomics and its potential in biodosimetry. *Int. J. Radiat. Biol.* **87**, 802–823 (2011)
7. Coy, S.L., Krylov, E.V., Schneider, B.B., Covey, T.R., Brenner, D.J., Tyburski, J.B., Patterson, A.D., Krausz, K.W., Fornace Jr., A.J., Nazarov, E.G.: Detection of radiation-exposure biomarkers by differential mobility prefiltered mass spectrometry (DMS-MS). *Int. J. Mass Spectrom.* **291**, 108–117 (2010)
8. Pannkuk, E.L., Laiakis, E.C., Authier, S., Wong, K., Fornace Jr., A.J.: Global metabolomic identification of long-term dose-dependent urinary biomarkers in nonhuman primates exposed to ionizing radiation. *Radiat. Res.* **184**, 121–133 (2015)
9. Goudarzi, M., Weber, W.M., Mak, T.D., Chung, J., Doyle-Eisele, M., Melo, D.R., Brenner, D.J., Guilmette, R.A., Fornace Jr., A.J.: Metabolomic and lipidomic analysis of serum from mice exposed to an internal emitter, cesium-137, using a shotgun LC-MSE approach. *J. Proteome Res.* **14**, 374–384 (2015)
10. Goudarzi, M., Weber, W.M., Chung, J.J., Doyle-Eisele, M., Melo, D.R., Mak, T.D., Strawn, S.J., Brenner, D.J., Guilmette, R., Fornace, A.J.: Serum dyslipidemia is induced by internal exposure to strontium-90 in mice, lipidomic profiling using a data-independent liquid chromatography-mass spectrometry approach. *J. Proteome Res.* **14**, 4039–4049 (2015)
11. Goudarzi, M., Weber, W.M., Mak, T.D., Chung, J.J., Doyle-Eisele, M., Melo, D.R., Strawn, S.J., Brenner, D.J., Guilmette, R.A., Fornace, A.J.: A comprehensive metabolomic investigation in urine of mice exposed to strontium-90. *Radiat. Res.* **183**, 665–674 (2015)
12. Laiakis, E.C., Trani, D., Moon, B.H., Strawn, S.J., Fornace, A.J.: Metabolomic profiling of urine samples from mice exposed to protons reveals radiation quality and dose specific differences. *Radiat. Res.* **183**, 382–390 (2015)
13. Mak, T.D., Tyburski, J.B., Krausz, K.W., Kalinich, J.F., Gonzalez, F.J., Fornace, A.J.: Exposure to ionizing radiation reveals global dose- and time-dependent changes in the urinary metabolome of rat. *Metabolomics* **11**, 1082–1094 (2015)
14. Laiakis, E.C., Strassburg, K., Bogumil, R., Lai, S., Vreeken, R.J., Hankemeier, T., Langridge, J., Plumb, R.S., Fornace, A.J., Astarita, G.: Metabolic phenotyping reveals a lipid mediator response to ionizing radiation. *J. Proteome Res.* **13**, 4143–4154 (2014)
15. Want, E.J., Cravatt, B.F., Siuzdak, G.: The expanding role of mass spectrometry in metabolite profiling and characterization. *Chem. Biochem.* **6**, 1941–1951 (2005)
16. Issaq, H.J., Abbott, E., Veenstra, T.D.: Utility of separation science in metabolomic studies. *J. Sep. Sci.* **31**, 1936–1947 (2008)
17. Schauer, N., Steinhäuser, D., Strelkov, S., Schomburg, D., Allison, G., Moritz, T., Lundgren, K., Roessner-Tunali, U., Forbes, M.G., Willmitzer, L., Fernie, A.R., Kopka, J.: GC-MS libraries for the rapid identification of metabolites in complex biological samples. *FEBS Lett.* **579**, 1332–1337 (2005)
18. Johnson, C.H., Patterson, A.D., Krausz, K.W., Kalinich, J.F., Tyburski, J.B., Kang, D.W., Luecke, H., Gonzalez, F.J., Blakely, W.F., Idle, J.R.: Radiation metabolomics. 5. Identification of urinary biomarkers of ionizing radiation exposure in nonhuman primates by mass spectrometry-based metabolomics. *Radiat. Res.* **178**, 328–340 (2012)
19. Johnson, C.H., Patterson, A.D., Krausz, K.W., Lanz, C., Kang, D.W., Luecke, H., Gonzalez, F.J., Idle, J.R.: Radiation metabolomics. 4. UPLC-ESI-QTOFMS-based metabolomics for urinary biomarker discovery in gamma-irradiated rats. *Radiat. Res.* **175**, 473–484 (2011)
20. Lanz, C., Patterson, A.D., Slavik, J., Krausz, K.W., Ledermann, M., Gonzalez, F.J., Idle, J.R.: Radiation metabolomics. 3. Biomarker discovery in the urine of gamma-irradiated rats using a simplified metabolomics protocol of gas chromatography-mass spectrometry combined with random forests machine learning algorithm. *Radiat. Res.* **172**, 198–212 (2009)
21. Tyburski, J.B., Patterson, A.D., Krausz, K.W., Slavik, J., Fornace Jr., A.J., Gonzalez, F.J., Idle, J.R.: Radiation metabolomics. 1. Identification of minimally invasive urine biomarkers for gamma-radiation exposure in mice. *Radiat. Res.* **170**, 1–14 (2008)
22. Tyburski, J.B., Patterson, A.D., Krausz, K.W., Slavik, J., Fornace Jr., A.J., Gonzalez, F.J., Idle, J.R.: Radiation metabolomics. 2. Dose- and time-dependent urinary excretion of deaminated purines and pyrimidines after sublethal gamma-radiation exposure in mice. *Radiat. Res.* **172**, 42–57 (2009)
23. Hall, A.B., Coy, S.L., Nazarov, E., Vouros, P.: Development of rapid methodologies for the isolation and quantitation of drug metabolites by differential mobility spectrometry-mass spectrometry. *Int. J. Ion Mobil. Spectrom.* **15**, 151–156 (2012)
24. Blagojevic, V., Chramow, A., Schneider, B.B., Covey, T.R., Bohme, D.K.: Differential mobility spectrometry of isomeric protonated dipeptides: modifier and field effects on ion mobility and stability. *Anal. Chem.* **83**, 3470–3476 (2011)
25. Shvartsburg, A.A., Creese, A.J., Smith, R.D., Cooper, H.J.: Separation of a set of peptide sequence isomers using differential ion mobility spectrometry. *Anal. Chem.* **83**, 6918–6923 (2011)
26. Kaffle, A., Klaene, J., Hall, A.B., Glick, J., Coy, S.L., Vouros, P.: A differential mobility spectrometry/mass spectrometry platform for the rapid detection and quantitation of DNA adduct dG-ABP. *Rapid Commun. Mass Spectrom.* **27**, 1473–1480 (2013)
27. Kaffle, A., Coy, S.L., Wong, B.M., Fornace Jr., A.J., Glick, J.J., Vouros, P.: Understanding Gas Phase Modifier Interactions in Rapid Analysis by Differential Mobility-Tandem Mass Spectrometry. *J. Am. Soc. Mass Spectrom.* **25**, 1098–1113 (2014)
28. Schneider, B.B., Covey, T.R., Coy, S.L., Krylov, E.V., Nazarov, E.G.: Planar differential mobility spectrometer as a pre-filter for atmospheric pressure ionization mass spectrometry. *Int. J. Mass Spectrom.* **298**, 45–54 (2010)
29. Laiakis, E.C., Hyduke, D.R., Fornace, A.J.: Comparison of mouse urinary metabolic profiles after exposure to the inflammatory stressors gamma radiation and lipopolysaccharide. *Radiat. Res.* **177**, 187–199 (2012)
30. Randall, K.L., Argoti, D., Paonessa, J.D., Ding, Y., Oaks, Z., Zhang, Y., Vouros, P.: An improved liquid chromatography-tandem mass spectrometry method for the quantification of 4-aminobiphenyl DNA adducts in urinary bladder cells and tissues. *J. Chromatogr. A* **1217**, 4135–4143 (2010)
31. Levin, D.S., Miller, R.A., Nazarov, E.G., Vouros, P.: Rapid separation and quantitative analysis of peptides using a new nanoelectrospray-differential mobility spectrometer-mass spectrometer system. *Anal. Chem.* **78**, 5443–5452 (2006)
32. Levin, D.S., Vouros, P., Miller, R.A., Nazarov, E.G.: Using a nanoelectrospray-differential mobility spectrometer-mass spectrometer system for the analysis of oligosaccharides with solvent selected control over ESI aggregate ion formation. *J. Am. Soc. Mass Spectrom.* **18**, 502–511 (2007)
33. Levin, D.S., Vouros, P., Miller, R.A., Nazarov, E.G., Morris, J.C.: Characterization of gas-phase molecular interactions on differential mobility ion behavior utilizing an electrospray ionization-differential mobility-mass spectrometer system. *Anal. Chem.* **78**, 96–106 (2006)
34. Schneider, B.B., Covey, T.R., Coy, S.L., Krylov, E.V., Nazarov, E.G.: Chemical Effects in the Separation Process of a Differential Mobility/Mass Spectrometer System. *Anal. Chem.* **82**, 1867–1880 (2010)
35. Krylov, E., Coy, S., Vandermeij, J., Schneider, B., Covey, T., Nazarov, E.: Selection and generation of waveforms for differential mobility spectrometry. *Rev. Sci. Instrum.* **81**, 024101 (2010)
36. Nazarov, E.G., Coy, S.L., Krylov, E.V., Miller, R.A., Eiceman, G.A.: Pressure effects in differential mobility spectrometry. *Anal. Chem.* **78**, 7697–7706 (2006)
37. Krylov, E.V., Coy, S.L., Nazarov, E.G.: Temperature effects in differential mobility spectrometry. *Int. J. Mass Spectrom.* **279**, 119–125 (2009)
38. Pannkuk, E.L., Laiakis, E.C., Mak, T.D., Astarita, G., Authier, S., Wong, K., Fornace, A.J.: A lipidomic and metabolomic serum signature from nonhuman primates exposed to ionizing radiation. *Metabolomics* **12**, 1–11 (2016)
39. Rose, C., Parker, A., Jefferson, B., Cartmell, E.: The characterization of feces and urine: a review of the literature to inform advanced treatment technology. *Crit. Rev. Environ. Sci. Technol.* **45**, 1827–1879 (2015)
40. Covey, T.R., Thomson, B.A., Schneider, B.B.: Atmospheric pressure ion sources. *Mass Spectrom. Rev.* **28**, 870–897 (2009)
41. Schneider, B.B., Covey, T.R., Coy, S.L., Krylov, E.V., Nazarov, E.G.: Control of chemical effects in the separation process of a differential mobility mass spectrometer system. *Eur. J. Mass Spectrom.* **16**, 57–71 (2010)

42. Schneider, B.B., Nazarov, E.G., Covey, T.R.: Peak capacity in differential mobility spectrometry: effects of transport gas and gas modifiers. *Int. J. Ion Mobil. Spectrom.* **15**, 141–150 (2012)
43. Barcenas, M., Suhr, T.R., Scott, C.R., Turecek, F., Gelb, M.H.: Quantification of sulfatides in dried blood and urine spots from metachromatic leukodystrophy patients by liquid chromatography/electrospray tandem mass spectrometry. *Clin. Chim. Acta* **433**, 39–43 (2014)
44. Carreno Balcazar, J.S., Meesters, R.J.W.: Bioanalytical comparison between dried urine spots and liquid urine bioassays used for the quantitative analysis of urinary creatinine concentrations. *Bioanalysis* **6**, 2803–2814 (2014)
45. Otero-Fernandez, M., Angel Cocho, J., Jesus Tabernero, M., Maria Bermejo, A., Bermejo-Barrera, P., Moreda-Pineiro, A.: Direct tandem mass spectrometry for the simultaneous assay of opioids, cocaine and metabolites in dried urine spots. *Anal. Chim. Acta* **784**, 25–32 (2013)
46. US-FDA: Guidance for Industry: Bioanalytical method validation. [ucm070107.pdf](#). (2001)
47. US-FDA: Guidelines for the Validation of Chemical Methods. [UCM298730.pdf](#). (2015)
48. Carayol, M., Licaj, I., Achaintre, D., Sacerdote, C., Vineis, P., Key, T.J., Onland Moret, N.C., Scalbert, A., Rinaldi, S., Ferrari, P.: Reliability of serum metabolites over a two-year period: a targeted metabolomic approach in fasting and non-fasting samples from EPIC. *PLoS One* **10**, e0135437 (2015)
49. Mak, T.D., Laiakis, E.C., Goudarzi, M., Fornace, A.J.: MetaboLyzer: a novel statistical workflow for analyzing postprocessed LC-MS metabolomics data. *Anal. Chem.* **86**, 506–513 (2014)
50. Mak, T.D., Laiakis, E.C., Goudarzi, M., Fornace, A.J.: Selective paired ion contrast analysis: a novel algorithm for analyzing postprocessed LC-MS metabolomics data possessing high experimental noise. *Anal. Chem.* **87**, 3177–3186 (2015)